Electrochemical oxidation of phosphatidylethanolamines studied by mass spectrometry

Simone Colombo[1,] Giulia Coliva[2,3], Agnieszka Kraj[4], Jean-Pierre Chervet[4], Maria Fedorova[2,3], Pedro Domingues[1] and M. Rosário Domingues[1]

[1]Mass Spectrometry Centre, Department of Chemistry & QOPNA, University of Aveiro, Campus Universitário de Santiago, 3810-193 Aveiro, Portugal

[2]Institute of Bioanalytical Chemistry, Faculty of Chemistry and Mineralogy, Universität Leipzig,

[3]Center for Biotechnology and Biomedicine, Universität Leipzig, Germany.

[4] Antec Scientific, Zoeterwoude, Netherlands

Corresponding author: M. Rosário Domingues[1]

Address reprint requests to: M Rosario M Domingues, Lipidomic laboratory, Departamento de Química, Universidade de Aveiro, Campus Universitário de Santiago, 3810-193 Aveiro (PORTUGAL)

Phone: +351 234 370698

Fax: +351 234 370084

E-mail: mrd@ua.pt

Abstract:

Phosphatidylethanolamines (PEs) are widely present in cellular membranes and lipoproteins. Oxidation of PEs fatty acyl chains generates several oxidized products, exerting a vast number of biological functions, not totally unveiled yet. *In vitro* biomimetic models have been used to identify oxidized PEs and to develop analytical strategies for their targeted detection *in vivo*. Most of the models are based on oxidation by reactive oxygen species (ROS), but the oxidative metabolism of PE also relies on controlled reactions catalyzed by enzymes as lipoxygenase (LOX), which can be mimicked by electrochemical (EC) oxidation. In this study, three PE standards (POPE, PLPE, and PAPE) were oxidized by EC oxidation, using an EC flow-through cell system as a biomimetic model of oxidative injury. The new oxidation products were identified by on-line EC-electrospray ionization mass spectrometry (EC-ESI-MS and MS/MS). Long chain and short chain oxidation products were identified, bearing modifications in the *sn*-2 acyl chains, whereas the oxidation pattern was dependent on the unsaturation level. Long chain oxidation products of PEs (keto, hydroxy, hydroperoxy, poly-hydroperoxy derivatives) were identified, bearing up to 5, 7 and 10 oxygens for POPE, PLPE and PAPE, respectively. Fourteen short chain oxidation products, seven from PLPE and seven from PAPE, including aldehydes, γ-hydroxy-α,β-aldehydes and dicarboxylic acids were characterized. Some of these oxidized species were previously reported during the oxidative metabolism of PEs driven by ROS. The EC-ESI-MS platform was, therefore, able to mimic the oxidative metabolism of PEs mediated by ROS.

Keywords: phospholipids, phosphatidylethanolamine, oxidation, electrochemistry, mass spectrometry

Introduction

Phospholipids are main constituents of the cellular membrane, mediating structural changes and signaling responses, including fluidity, water impermeability, intercellular communication and anchorage of signaling macromolecules.[1] Phospholipids also act as a pool of structures that can be modified to generate several signaling mediators.[2,3] Phosphatidylethanolamine (PE) is the second most abundant phospholipid class, contributing to around 20 % of the phospholipidome, being present in cell membranes and lipoproteins of mammalian organisms.[4] It is well known that phospholipid properties are affected by oxidation of the fatty acyl chains, whereas the degree of unsaturation is a factor that directly modulates the course of this structural modification.[5] The oxidation process leads to structurally diversified oxidized products that may lose their original function or exert new biological activities, different from those of the native phospholipid.[6–10] Phosphatidylcholine (PC) was the first phospholipid class characterized by mass spectrometry (MS) in terms of structure[11,12] and tendency to oxidize, hence several reviews comprehensively report the state of the art in the analysis of PC oxidized derivatives.[9,10,13] Differently, MS-based studies of oxidized PE have mainly been performed in the last decade,[10] and only few MS approaches aimed to the structural characterization of modified PE through reactive oxygen species (ROS) generating systems have so far been reported,[14–18] despite the role that oxidized PE may play in pathophysiologic processes. Biological functions of oxidized PE in mammalian cells include the modulation the of the immune system,[19–21] regulation of the mitogen-activated protein kinase (MAPK) pathway[22] and pro-coagulant activity mediated either via thrombin generation [23,24] or protein C inhibitor (PCI) modulation.[25]

PE can be oxidized by radical/non-enzymatic pathways or by enzyme-catalyzed reactions, with both mechanisms leading to diversified oxidation products.[26] ROS modify the unsaturated fatty acyl chains of PE by oxygen insertions and chain-decomposition

reactions.[5–7,9,10]However, a controlled cellular oxidation is fundamental for redox homeostasis, and many distinct physiological functions involve ROS as signaling molecules.[27] Figure 1 shows the mechanism of phospholipid peroxidation initiated by radical ROS on PAPE, and evidences the evolution of the process through the main oxidation products.

Enzymatic oxidation of PE in mammalian cells can also be mediated by conserved enzymes that catalyze stereospecific oxygen insertions on the unsaturated fatty acyl chains, upon controlled intracellular signaling pathways.[2,3,28] Unsaturated fatty acid chains that are usually esterified to the *sn*-2 position of the glycerol backbone of PE (e.g. linoleic acid, LA and arachidonic acid, AA) are metabolized *in vivo* to a wide range of oxidized lipids mediating biological functions related to inflammation, immunity, and regulation of cell growth.[29–32] The oxidative metabolism of LA, AA and other unsaturated lipids relies on cyclo-oxygenase (COX), cytochrome P450 (CYP450) and lipoxygenase (LOX).[28] LOXs are stereospecific dioxygenases, which catalyze the insertion of molecular oxygen into unsaturated fatty acids that bear at least one (1Z,4Z)-pentadiene system. The primary oxidation product of LOX catalysis is a lipid hydroperoxide that is intracellularly reduced to the corresponding lipid hydroxide by glutathione peroxidase (GPX).[3] Lipid oxidation derivatives produced by the catalysis of LOX and other enzymes have already been characterized by several studies that have mainly focused on the oxidation of free fatty acids, and this area of investigation has been reviewed.[28] More recently, the importance of enzymatic oxidation has been highlighted for the metabolism of PE-esterified lipids. Especially after the advances in high sensitivity mass spectrometry, several oxidized PEs produced by LOX-catalyzed reactions have been detected by targeted MS approaches in activated platelets,[2,3,24,33,34] neutrophils,[2,3,35] and monocytes/macrophages.[2,3,19,33,36] These studies on enzymatically oxidized PEs have shown how LOX can oxidize PE through two

pathways: (i) direct oxidation of PE,[19,33,36] (ii) oxidation of a free fatty acid released from the membrane PE pool, which is later re-esterified to generate the oxidized PE.[24,34,35]

PE oxidation has therefore been reported to occur as result of enzymatic and non-enzymatic pathways, and in both cases, the *in vivo* occurrence of the oxidized products has been suggested. Nowadays, the study of enzymatic and non-enzymatic oxidation mechanisms should start from *in vitro* biomimetic systems, able to predict the reactions that normally lead to the production of oxidized PE. In these biomimetic approaches, the oxidized PE species can be identified by MS and the fragmentation patterns studied by tandem MS, aiming to find diagnostic fragment ions for targeted *in vivo* analysis.[15–18] Facing a great variability of possible oxidation derivatives, an ideal biomimetic tool should be able to mimic as much as possible the oxidation chemistry that is likely to occur *in vivo*. Electrochemical (EC) oxidation coupled to electrospray ionization-mass spectrometry (ESI-MS) is both a micro-preparative and analytical platform that has been employed as a biomimetic model for studies aimed to simulate phase I and phase II drug metabolism[37] and to predict the oxidative modifications in biomolecules as nucleic acids, peptides, and proteins.[38] Some studies have reported the application of EC-ESI-MS in the prediction of the oxidative modifications of fatty acid methyl esters (FAME)[39] and cholesterols.[40] Nonetheless, the literature does not report any study in which this platform has been used for profiling the oxidation of phospholipids. In the present study, electrochemically induced modifications in the PE species POPE (16:0/18:1), PLPE (16:0/18:2) and PAPE (16:0/20:4) were identified by MS and characterized by MS/MS for a structural elucidation of the products. EC-ESI-MS is proposed as an innovative and technically simple tool for mimicking the oxidative metabolism of diversely unsaturated PEs within short times of reaction and analysis.

Experimental

Reagents/Chemicals

Phospholipid standards 1-palmitoyl-2-oleoyl-sn-glycero-3-phosphoethanolamine (POPE), 1-palmitoyl-2-linoleoyl-sn-glycero-3-phosphoethanolamine (PLPE) and 1-palmitoyl-2-arachidonoyl-sn-glycero-3-phosphoethanolamine (PAPE) were purchased from Avanti Polar Lipids, Inc. (Alabaster, AL, USA) and used without further purification. HPLC grade methanol and ammonium acetate for MS were purchased from Fisher Scientific (Hampton, NH, USA). Milli-Q water (18.2 MΩ.cm) used for all experiments was obtained from a Barnstead Easypure II system (Thermo Fisher Scientific, Waltham, MA, USA).

Electrochemical Oxidation

The EC reactions were conducted in the ROXY EC system (Antec Scientific, Zoeterwoude, NL) consisting of the ROXY potentiostat for the control of the flow-through µ-PrepCell 2.0 supplied with a Magic Diamond™ working electrode (BDD: Boron Doped Diamond) and a Pd/H_2 reference electrode. Phospholipid standards were diluted to the final concentration of 25 µM in 1:1 MeOH:20 mM ammonium acetate (pH 7.4) and infused through the µ-PrepCell at a constant rate of 20 µL/min. During the reaction, the temperature of the ROXY EC system was constantly maintained at 37°C. The ROXY EC system was directly coupled to the ESI-HCT Ion Trap mass spectrometer. Firstly, the voltage-induced oxidation of the phospholipid standards was assessed applying a ramp of voltages between two preset potential values – from 0 V to 3.40 V - in steps of 20 mV/s (scan mode), hence allowing to optimize a voltage that resulted in a stable EC reaction. As an outcome of these optimization steps, each phospholipid standard was successively oxidized applying a static potential over the whole process: 3.00 V was selected for POPE and 2.50 V was selected for PLPE and PAPE.

Mass spectrometry

The extent of electrochemically-induced oxidative modification, the identification and the structural characterization of the new oxidation products were all monitored by negative mode and positive mode ESI-MS and MS/MS experiments, using a spherical high capacity (HCT plus) ion trap mass spectrometer (Bruker, Millerica, MA, USA). The sample flowing the through μ-PrepCell was directly infused in the ESI source at the rate of 20 μL/min, while the remaining ESI conditions were set as follows: electrospray voltage of 4.2 kV; capillary temperature of 300 °C; sheath gas pressure set to 20.00 psi; drying gas flow rate set to 5.00 SLPM. For automated MS/MS experiments, the ions exceeding a relative intensity threshold of 5% were selected from each full-scan mass spectrum for tandem MS (MS/MS) analysis using collision-induced dissociation (CID). MS/MS spectra were acquired with the following settings: Profile mode; isolation width 4.00 *m/z* units; collisional amplitude 1 V; fragmentation time of 40 ms. Redundant MS/MS measurements were avoided enabling a real-time active exclusion of previously analyzed precursor ions, with the conditions set as follows: 2 repeat counts, exclusion duration 20 min. Data acquisition and treatment of results were carried out with Compass Data Analysis (version 4.2) and Compass Data Analysis Viewer (version 4.2) (Bruker, Billerica, MA, USA).

Results

Three PE standards were electrochemically oxidized in an amperometric flow-through EC-cell (μ-PrepCell™) and the PE oxidation products were studied by coupling the EC system directly to the ESI-HCT-IT-MS, operating in both negative and positive ion modes. When the μ-PrepCell™ cell was off (non-oxidative conditions, thus before oxidation), only the unmodified PEs were identified in the ESI-MS spectra as $[M+H]^+$ ions at 718.6 (POPE), 716.5 (PLPE), 740.5 (PAPE) in the positive ion mode, and as $[M-H]^-$ ions at 716.5 (POPE),

714.4 (PLPE) and 738.5 (PAPE) in the negative ion mode. Comparison of the ESI-MS spectra of the PE standards before and after the application of the potential allowed the detection of remarkable changes in the mass spectra, both in the negative and in the positive ion mode. Full MS spectra acquired in negative ion mode for POPE, PLPE and PAPE before and after the EC oxidation are shown in Figure 2. For all the PEs, new ions generated by the EC treatment were observed at higher *m/z* values than the $[M-H]^-$ and the $[M+H]^+$ ions of the non-modified PEs. The new ions were identified as long chain oxidation products of PEs including keto, hydroxy, hydroperoxy and poly-hydroperoxy derivatives ($[M+nO]^+$, n = 1-5 for POPE; n = 1-7 for PLPE; n = 1-10 for PAPE), as summarized in Table 1 for the ions observed in positive mode, as $[M+H]^+$ ions (along with their relative abundances). All the long chain oxidation products reported in Table 1 were also identified in negative ion mode. For PLPE and PAPE, new ions also appeared at lower *m/z* values than the $[M-H]^-$ and the $[M+H]^+$ ions of the unmodified PEs and were identified as short chain oxidation products (Table 2). Short chain oxidation products were not observed for POPE. Full MS spectra acquired in negative ion mode for oxidized POPE, PLPE and PAPE are shown as an example in Figure 2. No oxidation products were identified below *m/z* 500. The structural elucidation of the new oxidation products was carried out by ESI-MS/MS analysis in positive and negative ion modes. In all the positive ion mode MS/MS of the oxidation products it was possible to observe the neutral loss of 141 Da (loss of the phosphoethanolamine polar head). This is a typical neutral loss of PE in positive ion mode, [12] which confirmed that the assigned products were oxidized PEs and that the oxidation did not occurred in the polar head. All the MS/MS spectra acquired in negative ion mode showed the typical fragmentation pathways of PEs.[12,17] These include the formation of carboxylate anions of the fatty acids esterified to the *sn-1* and *sn-2* positions, and the formation of ions due to losses of the modified fatty acyl chain from the *sn-2* position as ketene derivative ($-R_2=C=O$), with

192 formation lysoPE ions. In these MS/MS spectra of oxidized PE, it was therefore always
193 possible to identify the typical carboxylate ion, R_1COO^-, of palmitic acid at *m/z* 255 (Figures
194 3, 4 and 5) which is not prone to oxidize. In addition, it is also possible to see the carboxylate
195 anions of the modified fatty acid at *sn-2* bearing several oxygen insertions (R'_2COO^-) that
196 allowed us to assign the modifications on the unsaturated fatty acyl chains. Furthermore, in
197 the MS/MS spectra, it was also possible to see the fragment ions due to loss of 18 Da (H_2O),
198 of 32 Da (O_2) and of 34 Da (H_2O_2) (Figures 3, 4 and 5), which have already been reported as
199 typical neutral losses typical of the hydroxy and hydroperoxy moieties in previous studies of
200 phospholipid oxidation.[15,41] The presence of the hydroperoxy moiety is strongly
201 corroborated from the neutral losses of 34 Da from the modified *sn-2* fatty acyl chains.
202 Interestingly, the combined losses of 32 Da plus 34 Da and loss of multiple 34 Da in the
203 MS/MS spectra can be used to confirm the presence of multiple hydroperoxy moieties. This
204 is shown in Figures 3, 4 and 5, using three PAPE oxidation products as examples, namely
205 hydroxy-hydroperoxy-PAPE, di-hydroperoxy-PAPE and keto-hydroxy-dihydroperoxy-PAPE
206 (Scheme 1, Panels A, B and C, respectively).

207 In the case of hydroxy-eicosatetraenoic acid-PE (HETE-PE or hydroxy-PAPE.
208 Scheme 1, Panel D), the MS/MS spectrum of the $[M-H]^-$ ion at *m/z* 754.4 showed a product
209 ion at *m/z* 319.0 attributed to the carboxylate anion of the hydroxy-AA, which corresponds to
210 the modified fatty acid in *sn-2*. This observation is characteristic and has been extensively
211 described for mono-hydroxylated phospholipids.[5,9] It was also possible to observe a product
212 ion at *m/z* 219.1, which was already been found to arise from the MS/MS fragmentation of
213 the 15-HETE-PE, a PE oxidation product bearing one hydroxyl group at C15, formed
214 enzymatically by 15-LOX).[36,42] However, the presence of other positional isomers, with
215 hydroxide/hydroperoxide moieties inserted on other carbons are also possible, as mentioned
216 before. When performing a structural characterization of oxidation products of PE by

MS/MS, it is difficult to propose possible locations for the functional groups along the fatty acyl chains, since multiple position of oxygenated structures for sure occur.[15]

The MS/MS spectrum of the $[M-H]^-$ of hydroxy-hydroperoxy-PAPE at *m/z* 786.5 (Figure 3) shows the product ion at *m/z* 351.1, correspondent to the carboxylate ion of the oxidized AA at *sn-2* (hydroxy-hydroperoxy-AA) bearing three oxygen insertions (303 + 48 Da). The neutral loss of the modified fatty acid as ketene produced the ion at *m/z* 452.1. The product ion at *m/z* 754.4 is due to the neutral loss of O_2 (-32 Da), which has already been reported to occur for hydroperoxy derivatives of phospholipids.[15,41] Furthermore, the fragment at *m/z* 768.4, arising from the neutral loss of H_2O (-18 Da), confirmed the presence of one hydroxy moiety on the AA fatty acyl chain.[15,41] Since the MS/MS spectra of the ion at *m/z* 786.5 reported intense neutral losses of O_2 and H_2O, we identified this ion as a hydroxy-hydroperoxy-PAPE. In the context of the analysis of PLPE bearing 2 oxygen insertions (PLPE+2O), it was previously observed that the typical fragmentation of hydroperoxide moieties under MS/MS displays abundant ions due to loss of H_2O_2 (-34 Da) and /or O_2 (-32 Da). [15] The neutral loss of H_2O_2 from the oxidized parent ion was also correlated with the insertion of hydroperoxide in several works reporting MS/MS analyzes of oxidized PCs.[43–46]. Additionally, the neutral loss of O_2 had already been proposed as a characteristic fingerprint of hydroperoxides moieties, in other studies focused on the structural characterization of oxidized phospholipids by MS/MS. [47,48] In contrast, in poly-hydroxy derivatives these products of fragmentation are absent and the MS/MS spectra are characterized by abundant losses of one H_2O molecule (-18 Da) and losses of multiple H_2O molecules (losses of n x 18 Da, such as loss of 36 Da and loss of 54 Da, that can occur in the case of more than 2 hydroxyl moieties).[41] These fragmentations by multiple losses of H_2O molecules are not abundant in the case of poly-hydroperoxy derivatives identified herin, as

we observed for the ion at *m/z* 786 (Figure 3). The coexistence with the isobaric tri-hydroxy-PAPE, however, cannot be excluded, since this species could be present in minor amounts .

In the MS/MS spectrum of the $[M-H]^-$ ion of di-hydroperoxy-PAPE at *m/z* 802.5 (Figure 4) it is possible to observe the product ion at *m/z* 367.1, which corresponds to the carboxylate ion of the oxidized AA at *sn-2* (di-hydroperoxy-AA) bearing four oxygen insertions (303 + 64 Da), while it is possible to observe the loss of the modified *sn-2* fatty acid as ketene at *m/z* 452.1. The MS/MS spectrum also depicts the product ion at *m/z* 770.4 attributed to neutral loss of O_2 (-32 Da) and the product ion at *m/z* 736.2 arising from combined losses of O_2 (-32 Da) plus H_2O_2 (-34 Da), that confirms the presence of two hydroperoxy moieties on the AA fatty acyl chain. Altogether, the MS/MS spectrum of the ion at *m/z* 802.5 reports very intense product ions due to neutral losses of H_2O, O_2 and H_2O_2 that allowed us to identify this oxidation product as a di-hydroperoxy-PAPE. As discussed above for the ion at *m/z* 786, also in this case we did not observe abundant multiple neutral losses or H_2O in the MS/MS spectrum, however isobaric tetra-hydroxy-PAPE cannot be excluded and could be formed in minor amounts.

Figure 5 depicts the MS/MS spectrum of the $[M-H]^-$ ion of keto-hydroxy-dihydroperoxy-PAPE at *m/z* 832.5. The product ion at *m/z* 397.1 corresponds to the carboxylate ion of the oxidized AA bearing six oxygen insertions on the *sn-2* (303 + 94 Da, keto-hydroxy-dihydroperoxy -AA). Additionally, the loss of the modified fatty *sn-2* acid as ketene can be observed through the product ion at *m/z* 452.1. We have also observed the product ion at *m/z* 814.4 due to the neutral loss of one H_2O molecule (-18 Da) from the single hydroxyl moiety, and the product ion at *m/z* 800.4 (-32 Da) resulting from one of the two hydroperoxyl moieties. Finally, the product ion at *m/z* 736.2 arises from the multiple loss of two O_2 molecules (-64 Da), that is related to the presence of two hydroperoxyl moieties on the AA fatty acyl chain. Considering that this MS/MS spectrum reports an evident neutral

loss of H_2O plus a single and a multiple neutral loss of molecular oxygen, we characterized this molecule as keto-hydroxy-dihydroperoxy-PAPE.

As stated for mono-hydroxy-PAPE, proposing a location of the oxygenated functional groups along the chain based on the MS/MS structural characterization is a difficult task: particularly in the case of poly-oxygenated long chain oxidation products as the ions at *m/z* 786.5, *m/z* 802.5 and *m/z* 832.5, it becomes even more challenging to determine straightforwardly the positional isomers within the mixture.[15] Hence, the long chain oxidation products of PAPE showed in Scheme 1 are represented without a definitive assignation of the carbon atoms bearing the oxygen insertions.

Since the MS/MS spectra were acquired with the ion trap mass spectrometer upon collision-induced dissociation (CID), we were only able to acquire fragmentation spectra in which the lowest *m/z* value of the product ions corresponded to 1/3 of the *m/z* of the precursor ion (low-mass cutoff). Thus, in some cases, the carboxylate anions of the shortened fatty acyl chains of short chain oxidation products cannot be seen. In this case, MS/MS in positive mode can be used for the structural characterization of short-chain oxidation products, as exemplified for the ion at *m/z* 552.3, a short chain oxidation product of PAPE (Figure 6). The fragmentation of this ion upon positive ion mode MS/MS yields a base peak at *m/z* 411.3 that arises from the neutral loss of the phosphoethanolamine polar head (-141 Da) and confirms that the short chain oxidized molecule is a modified PE. Another important product ion can be observed at *m/z* 313.3, which is attributable to the combined neutral loss of 141 Da and of the modified and shortened *sn-2* acyl chain. The product ion at *m/z* 534.3 results from the neutral loss of H_2O from the aldehyde group. Upon the whole, these observations confirmed the presence of a shortened *sn-2* fatty acid bearing an aldehyde moiety, thus allowing us to assign the ion at *m/z* 552.3 as 1-(palmitoyl)-2-(5-oxopentanoyl)-PE.

Discussion

Using an amperometric flow-through EC-cell (µ-PrepCell™) supplied with a Magic Diamond™ working electrode (BDD: Boron Doped Diamond) and a Pd/H_2 reference electrode, we electrochemically oxidized the three PE molecular species POPE (16:0/18:1), PLPE (16:0/18:2) and PAPE (16:0/20:4), and we analyzed the oxidized mixture by on-line direct infusion ESI-MS and MS/MS. The EC device employed in this study worked with a BDD electrode that mediates an anodic oxidation of H_2O, leading to the abstraction of one electron from the H_2O molecules and to the production of ·OH.[37] Thus, ·OH is the ROS that mediated the oxidation of the organic compounds in the BDD-equipped EC cells.[37] Based on this knowledge, we used EC oxidation as a biomimetic model of ·OH-induced oxidation of PEs. The online EC-MS and MS/MS system allowed the identification and the characterization of the oxidized products in few minutes, which is a great advantage considering the time of reaction of several days needed for the majority of the other oxidation systems. Comparison of the ESI-MS spectra of the PE standards before and after the application of the potential allowed the detection of new ions at higher *m/z* values than the $[M-H]^-$ and the $[M+H]^+$ of the unmodified PEs. We identified these ions as long chain oxidation products of PEs as keto, hydroxy, hydroperoxy and poly-hydroperoxy derivatives (in the positive ion mode: $[M+H + nO]^+$, n = 1-5 for POPE; n = 1-7 for PLPE; n = 1-10 for PAPE) (Table 1). In terms of relative intensity, the data reported in Table 1 shows that the most abundant oxidized species for POPE and PLPE were the mono-hydroxy and the mono-hydroperoxy derivative, respectively. Differently, the most intense oxidation product of PAPE has been identified as tri-hydroperoxy-PAPE. These results are in agreement with the principles of lipid peroxidation, whereas the unsaturation level correlates with the number of inserted oxygen atoms.[5,49] The EC cell was employed in the present work as a biomimetic method of oxidation induced by ·OH, which was the effector of the radical peroxidation

observed for the PE standards. Oxidation of PE by ·OH generated by Fenton reaction was already reported by Domingues et al.[15] and Simões et al.[16] Domingues et al.[15] studied the oxidation of PLPE induced with the Fenton reaction, observing the formation of long-chain oxidation products bearing up to 4 oxygens (PLPE + 4O), along with 11 short chain oxidation products with terminal aldehyde and carboxylic acid. Hence, the authors observed a lesser extent of long chain products and a higher number of short chain derivatives in comparison with the present work (1 to 7 oxygen insertions and 7 short chain oxidation products observed for PLPE). In the same work, the ion of PLPE + 2O was found to be the most intense in the ESI-MS spectrum acquired in the positive ion mode, similarly to what we observed in our study.[15] Likely to what we observed in our experiments, the long chain oxidation products identified in the previous studies included keto-PLPE, keto-hydroxy-PLPE, hydroxy-PLPE and hydroxy-hydroperoxy-PLPE.[15,16] However, the EC-ESI-MS platform has the advantage to allow the formation and the direct analysis the oxidized species within minutes and without the need of any further protocol of lipid extraction. Additionally, the long chain oxidation products of POPE and PLPE were formed with a higher number of hydroperoxyl moieties, when compared with the results of oxidative treatments to PEs induced by photosensitization[17,18] or Fenton reaction.[15,16] Hence, even though the radical-based mechanism of peroxidation induced by EC led to the same oxidation products observed for Fenton, we noticed a remarkable difference in the extent of the oxidation mediated by the EC cell. A high extent of oxygen insertion was also reported for the EC-mediated oxidation of cholesterol[40] and fatty acids methyl esters (FAMEs) of biodiesel.[39] The potential applied to the EC cell induces one-electron abstractions from H_2O molecules on the electron surface.[37] The hydroxyl radical (·OH) generated by this abstraction is the oxidizing agent in the cell, produced within different times and quantities depending on the cell potential (2.50 or 3.00 V in the present work).[37] Hence, the redox potential of the one-electron abstraction occurring in

this system corresponds to the one-electron redox potential of the $\cdot OH,H^+/H_2O$ couple relatively to the standard hydrogen electrode (SHE) ($E^0_{\cdot OH,H+/H2O}$ = 2.30 V as measured by Buettner,[50] $E^0_{\cdot OH,H+/H2O}$ = 2.80 V as reviewed by Brillas et al.[51]). The Fenton system also leads to the production of ·OH, therefore the same one-electron redox potential ($E^0_{\cdot OH,H+/H2O}$) is expected during this reaction.[50,51] We assume that the main reason for the higher number of oxygen insertions that we observed here is the fast and extensive production of ·OH, generated in the EC cell on the electrode surface, which is a peculiar feature of this on-line EC-ESI-MS system. However, this extended oxidation pattern might also be due to the very short time elapsing through the production and the analysis of the oxidized products, that is another feature achieved by the on-line analysis.

The structural elucidation of the long chain oxidation products highlighted a direct correlation between the number of oxygens added to the unsaturated fatty acyl chains and their number of unsaturations, as normally observed for radical-driven oxidation of phospholipids.[5] These observations are consistent with the radical oxidation mechanism mediated by the EC cell:[37] ·OH generated under electrochemical oxidation conditions leads to the formation of carbon-centered radicals on the unsaturated fatty acyl chains. These carbon-centered radicals react with O_2 to generate the hydroperoxyl radical, as typically reported for lipid peroxidation.[5] Within the present work, the EC cells operated at atmospheric pressure, thus O_2 was available for the reaction. In the case of poly-hydroperoxy-PEs, we performed a structural characterization based on the neutral losses of O_2 (-32 Da) and H_2O_2 (-34 Da) in the MS/MS spectra. We observed that:

(i) The number of sequential O_2 and H_2O_2 neutral losses in the MS/MS spectra depends on the number of hydoperoxyl moieties that have been inserted into the *sn-2* fatty acyl chain;

(ii) The absence of multiple neutral losses of H_2O in the MS/MS spectra of a (poly)hydroperoxy-PE can be used to distinguish it by an isobaric polyhydroxy-PE;

(iii) The co-insertion on the fatty acyl chain of hydroperoxyl groups and further oxygen moieties (keto, hydroxyl) does not hinder the observance of the typical hydroperoxy-diagnostic neutral losses (-32 Da, -34 Da) in the MS/MS fragmentation pattern.

Among the mixture of oxidized derivatives produced in the EC cell, we identified as most abundant the mono-hydroxy-PEs and mono-hydroperoxy-PEs, which were reported before to be formed either by metal-catalyzed oxidation, usually mediated by the hydroxyl radical[10,15] and also by oxidative metabolism of PE-mediated by the enzyme lipoxygenase (LOX) *in vivo*.[52] We found that mono-hydroxy-PE and mono-hydroperoxy-PE were the most intense ions in the mixtures of oxidized POPE and oxidized PLPE, respectively. Mono-hydroxy-PE and mono-hydroperoxy-PE were also identified among the oxidized PAPE derivatives, despite the most intense oxidized products in the correspondent full MS spectra arose from the poly-hydroperoxy species (+4O, +5O, +6O). Mono-hydroperoxy-PAPE belongs to a group of oxidized species named hydroperoxy-eicosatetraenoic-PEs (HPETE-PEs). Herein, through the EC-ESI-MS platform it was possible to generate and characterize the hydroperoxy and the hydroxy derivatives for all the three PE species (POPE, PLPE, and PAPE), and their fragmentation fingerprinting. These observations highlighted the potential of the EC-ESI-MS platform in mimicking ROS-mediated modification of PEs.

We were also able to elucidate the structure of 14 short chain oxidation products arising from the oxidation of PLPE and PAPE. The occurrence of short chain oxidation products has already been reported for *in vitro* models of ROS-mediated PEs oxidation. [15,53] Herein, the hydroperoxy groups on the fatty acyl chains degraded and led to the formation of

alkoxyl radicals, that underwent a β-cleavage of the C-C bond between the vinylic double bond and the substituted carbon atom, with the formation of chain-shortened aldehydes and carboxylic acids on the *sn-2* position.[5,15] Therefore, the number of carbon atoms of these esterified aldehydes/carboxylic acids can be related to the position of the oxygen atom in the fatty acyl chain that underwent the β-cleavage. These results pinpoint the power of EC-ESI-MS in predicting the oxidation products of PE occurring via radical-mediated oxidation *in vitro*. For POPE, no short chain oxidation products were observed, which is in accordance with the literature. To the best of our knowledge, there have not been reports on short chain oxidation products of phospholipids bearing oleic acid, which is in agreement with our observations for POPE electrochemical oxidation. The formation of short chain oxidation products has only been observed for phospholipid species bearing poly-unsaturated fatty acids.[15,16,53]

Conclusions

In this study, we submitted three PE molecular species (POPE, PLPE, and PAPE) to EC oxidation, and the oxidized products were identified and structurally characterized by ESI-MS/MS. Using this approach, we have identified long chain and short chain oxidation products due to the oxidative modification of the unsaturated fatty acyl chains, resulting from the PE oxidation mediated by the hydroxyl radical (·OH) generated in the EC cell. Among these products, it was possible to characterize the species mono-hydroperoxy-PAPE and the mono-hydroxy-PAPE, detected in human monocytes and macrophages and previously characterized in other studies performing *in vitro* analyzes of oxidized PE. EC oxidation and direct on-line analysis of the oxidized products by ESI-MS was, therefore, able to give information on PE metabolism of non-enzymatic, radical-driven PE oxidation. The online EC-ESI-MS platform has the great advantage of mimicking ROS-mediated reactions and predict extensive patterns of possible lipid modification in very fast reaction times, without the need of organic solvent-based extractions and time-consuming laboratory procedures.

Acknowledgments

Thanks are due to University of Aveiro, FCT/MEC, European Union, QREN, COMPETE for the financial support to the QOPNA (FCT UID/QUI/00062/2013), through national funds and where applicable co-financed by the FEDER, within the PT2020 Partnership Agreement, to the Portuguese Mass Spectrometry Network (REDE/1504/REM/2005), and to the funding from European Commission's Horizon 2020 research and innovation programme under the Marie Sklodowska-Curie grant agreement number 675132 (MSCA-ITN-ETN MASSTRPLAN).

References

[1] J. E. Vance, G. Tasseva. Formation and function of phosphatidylserine and phosphatidylethanolamine in mammalian cells. *Biochim. Biophys. Acta BBA - Mol. Cell Biol. Lipids* **2013**, *1831*, 543.

[2] V. B. O'Donnell, R. C. Murphy. New families of bioactive oxidized phospholipids generated by immune cells: identification and signaling actions. *Blood* **2012**, *120*, 1985.

[3] V. J. Hammond, V. B. O'Donnell. Esterified eicosanoids: Generation, characterization and function. *Biochim. Biophys. Acta BBA - Biomembr.* **2012**, *1818*, 2403.

[4] J. E. Vance. Thematic Review Series: Glycerolipids. Phosphatidylserine and phosphatidylethanolamine in mammalian cells: two metabolically related aminophospholipids. *J. Lipid Res.* **2008**, *49*, 1377.

[5] A. Reis, C. M. Spickett. Chemistry of phospholipid oxidation. *Biochim. Biophys. Acta BBA - Biomembr.* **2012**, *1818*, 2374.

[6] G. O. Fruhwirth, A. Loidl, A. Hermetter. Oxidized phospholipids: From molecular properties to disease. *Biochim. Biophys. Acta BBA - Mol. Basis Dis.* **2007**, *1772*, 718.

[7] V. N. Bochkov, O. V. Oskolkova, K. G. Birukov, A.-L. Levonen, C. J. Binder, J. Stöckl. Generation and biological activities of oxidized phospholipids. *Antioxid. Redox Signal.* **2010**, *12*, 1009.

[8] T. M. McIntyre, G. A. Zimmerman, S. M. Prescott. Biologically active oxidized phospholipids. *J. Biol. Chem.* **1999**, *274*, 25189.

[9] M. R. M. Domingues, A. Reis, P. Domingues. Mass spectrometry analysis of oxidized phospholipids. *Chem. Phys. Lipids* **2008**, *156*, 1.

[10] V. B. O'Donnell. Mass spectrometry analysis of oxidized phosphatidylcholine and phosphatidylethanolamine. *Biochim. Biophys. Acta BBA - Mol. Cell Biol. Lipids* **2011**, *1811*, 818.

[11] R. A. Klein. Mass spectrometry of the phosphatidylcholines: dipalmitoyl, dioleoyl, and stearoyl-oleoyl glycerylphosphorylcholines. *J. Lipid Res.* **1971**, *12*, 123.

[12] M. Pulfer, R. C. Murphy. Electrospray mass spectrometry of phospholipids. *Mass Spectrom. Rev.* **2003**, *22*, 332.

[13] C. M. Spickett, A. R. Pitt. Oxidative Lipidomics Coming of Age: Advances in Analysis of Oxidized Phospholipids in Physiology and Pathology. *Antioxid. Redox Signal.* **2015**, *22*, 1646.

[14] N. Khaselev, R. C. Murphy. Susceptibility of plasmenyl glycerophosphoethanolamine lipids containing arachidonate to oxidative degradation. *Free Radic. Biol. Med.* **1999**, *26*, 275.

[15] M. R. M. Domingues, C. Simões, J. P. da Costa, A. Reis, P. Domingues. Identification of 1-palmitoyl-2-linoleoyl-phosphatidylethanolamine modifications under oxidative stress conditions by LC-MS/MS. *Biomed. Chromatogr.* **2009**, *23*, 588.

[16] C. Simões, V. Simões, A. Reis, P. Domingues, M. R. M. Domingues. Oxidation of glycated phosphatidylethanolamines: evidence of oxidation in glycated polar head identified by LC-MS/MS. *Anal. Bioanal. Chem.* **2010**, *397*, 2417.

[17] T. Melo, N. Santos, D. Lopes, E. Alves, E. Maciel, M. A. F. Faustino, J. P. C. Tomé, M. G. P. M. S. Neves, A. Almeida, P. Domingues, M. A. Segundo, M. R. M. Domingues. Photosensitized oxidation of phosphatidylethanolamines monitored by electrospray tandem mass spectrometry: ESI-MS of photosensitized phosphatidylethanolamines. *J. Mass Spectrom.* **2013**, *48*, 1357.

[18] T. Melo, E. M. P. Silva, C. Simões, P. Domingues, M. R. M. Domingues. Photooxidation of glycated and non-glycated phosphatidylethanolamines monitored by mass spectrometry: Photooxidation of PE and GlucPE. *J. Mass Spectrom.* **2013**, *48*, 68.
[19] A. H. Morgan, V. Dioszeghy, B. H. Maskrey, C. P. Thomas, S. R. Clark, S. A. Mathie, C. M. Lloyd, H. Kuhn, N. Topley, B. C. Coles, P. R. Taylor, S. A. Jones, V. B. O'Donnell. Phosphatidylethanolamine-esterified Eicosanoids in the Mouse: TISSUE LOCALIZATION AND INFLAMMATION-DEPENDENT FORMATION IN Th-2 DISEASE. *J. Biol. Chem.* **2009**, *284*, 21185.
[20] C. Simões, A. C. Silva, P. Domingues, P. Laranjeira, A. Paiva, M. R. M. Domingues. Phosphatidylethanolamines Glycation, Oxidation, and Glycoxidation: Effects on Monocyte and Dendritic Cell Stimulation. *Cell Biochem. Biophys.* **2013**, *66*, 477.
[21] E. von Schlieffen, O. V. Oskolkova, G. Schabbauer, F. Gruber, S. Bluml, M. Genest, A. Kadl, C. Marsik, S. Knapp, J. Chow, N. Leitinger, B. R. Binder, V. N. Bochkov. Multi-Hit Inhibition of Circulating and Cell-Associated Components of the Toll-Like Receptor 4 Pathway by Oxidized Phospholipids. *Arterioscler. Thromb. Vasc. Biol.* **2009**, *29*, 356.
[22] J. Zhao, V. B. O'Donnell, S. Balzar, C. M. St. Croix, J. B. Trudeau, S. E. Wenzel. 15-Lipoxygenase 1 interacts with phosphatidylethanolamine-binding protein to regulate MAPK signaling in human airway epithelial cells. *Proc. Natl. Acad. Sci.* **2011**, *108*, 14246.
[23] S. Zieseniss, S. Zahler, I. Müller, A. Hermetter, B. Engelmann. Modified Phosphatidylethanolamine as the Active Component of Oxidized Low Density Lipoprotein Promoting Platelet Prothrombinase Activity. *J. Biol. Chem.* **2001**, *276*, 19828.
[24] C. P. Thomas, L. T. Morgan, B. H. Maskrey, R. C. Murphy, H. Kuhn, S. L. Hazen, A. H. Goodall, H. A. Hamali, P. W. Collins, V. B. O'Donnell. Phospholipid-esterified Eicosanoids Are Generated in Agonist-activated Human Platelets and Enhance Tissue Factor-dependent Thrombin Generation. *J. Biol. Chem.* **2010**, *285*, 6891.
[25] J. M. Malleier, O. Oskolkova, V. Bochkov, I. Jerabek, B. Sokolikova, T. Perkmann, J. Breuss, B. R. Binder, M. Geiger. Regulation of protein C inhibitor (PCI) activity by specific oxidized and negatively charged phospholipids. *Blood* **2007**, *109*, 4769.
[26] M. J. Davies. Protein oxidation and peroxidation. *Biochem. J.* **2016**, *473*, 805.
[27] W. Dröge. Free Radicals in the Physiological Control of Cell Function. *Physiol. Rev.* **2002**, *82*, 47.
[28] K. A. Massey, A. Nicolaou. Lipidomics of polyunsaturated-fatty-acid-derived oxygenated metabolites. *Biochem. Soc. Trans.* **2011**, *39*, 1240.
[29] W. Kim, N. A. Khan, D. N. McMurray, I. A. Prior, N. Wang, R. S. Chapkin. Regulatory activity of polyunsaturated fatty acids in T-cell signaling. *Prog. Lipid Res.* **2010**, *49*, 250.
[30] A. M. Sessler, J. M. Ntambi. Polyunsaturated fatty acid regulation of gene expression. *J. Nutr.* **1998**, *128*, 923.
[31] P. C. Calder. *Polyunsaturated Fatty Acids and Inflammation*. Portland Press Limited, **2005**.
[32] J. J. Moreno. New aspects of the role of hydroxyeicosatetraenoic acids in cell growth and cancer development. *Biochem. Pharmacol.* **2009**, *77*, 1.
[33] B. H. Maskrey, A. Bermudez-Fajardo, A. H. Morgan, E. Stewart-Jones, V. Dioszeghy, G. W. Taylor, P. R. S. Baker, B. Coles, M. J. Coffey, H. Kuhn, V. B. O'Donnell. Activated Platelets and Monocytes Generate Four Hydroxyphosphatidylethanolamines via Lipoxygenase. *J. Biol. Chem.* **2007**, *282*, 20151.

[34] L. T. Morgan, C. P. Thomas, H. Kühn, V. B. O'Donnell. Thrombin-activated human platelets acutely generate oxidized docosahexaenoic-acid-containing phospholipids via 12-lipoxygenase. *Biochem. J.* **2010**, *431*, 141.
[35] S. R. Clark, C. J. Guy, M. J. Scurr, P. R. Taylor, A. P. Kift-Morgan, V. J. Hammond, C. P. Thomas, B. Coles, G. W. Roberts, M. Eberl, others. Esterified eicosanoids are acutely generated by 5-lipoxygenase in primary human neutrophils and in human and murine infection. *Blood* **2011**, *117*, 2033.
[36] V. J. Hammond, A. H. Morgan, S. Lauder, C. P. Thomas, S. Brown, B. A. Freeman, C. M. Lloyd, J. Davies, A. Bush, A.-L. Levonen, E. Kansanen, L. Villacorta, Y. E. Chen, N. Porter, et al. Novel Keto-phospholipids Are Generated by Monocytes and Macrophages, Detected in Cystic Fibrosis, and Activate Peroxisome Proliferator-activated Receptor-. *J. Biol. Chem.* **2012**, *287*, 41651.
[37] H. Faber, M. Vogel, U. Karst. Electrochemistry/mass spectrometry as a tool in metabolism studies—A review. *Anal. Chim. Acta* **2014**, *834*, 9.
[38] S. Jahn, U. Karst. Electrochemistry coupled to (liquid chromatography/) mass spectrometry—Current state and future perspectives. *J. Chromatogr. A* **2012**, *1259*, 16.
[39] W. Ratsameepakai, C. Wicking, J. Herniman, S. Lambert, G. J. Langley. Hyphenation of On-line EC-ESI-TOF-MS: An Analytical Method for Monitoring FAME Oxidation. **n.d.**
[40] D. Weber, Z. Ni, D. Vetter, R. Hoffmann, M. Fedorova. Electrochemical oxidation of cholesterol: An easy way to generate numerous oxysterols in short reaction times: Characterization of electrochemically generated oxysterols. *Eur. J. Lipid Sci. Technol.* **2016**, *118*, 325.
[41] V. A. Tyurin, Y. Y. Tyurina, M.-Y. Jung, M. A. Tungekar, K. J. Wasserloos, H. Bayır, J. S. Greenberger, P. M. Kochanek, A. A. Shvedova, B. Pitt, V. E. Kagan. Mass-spectrometric analysis of hydroperoxy- and hydroxy-derivatives of cardiolipin and phosphatidylserine in cells and tissues induced by pro-apoptotic and pro-inflammatory stimuli. *J. Chromatogr. B* **2009**, *877*, 2863.
[42] M. Gulliksson, Å. Brunnström, M. Johannesson, L. Backman, G. Nilsson, I. Harvima, B. Dahlén, M. Kumlin, H.-E. Claesson. Expression of 15-lipoxygenase type-1 in human mast cells. *Biochim. Biophys. Acta BBA - Mol. Cell Biol. Lipids* **2007**, *1771*, 1156.
[43] J. Adachi, N. Yoshioka, R. Funae, H. Nushida, M. Asano, Y. Ueno. Determination of phosphatidylcholine monohydroperoxides using quadrupole time-of-flight mass spectrometry. *J. Chromatogr. B* **2004**, *806*, 41.
[44] J. Adachi, N. Yoshioka, M. Sato, K. Nakagawa, Y. Yamamoto, Y. Ueno. Detection of phosphatidylcholine oxidation products in rat heart using quadrupole time-of-flight mass spectrometry. *J. Chromatogr. B* **2005**, *823*, 37.
[45] C. M. Spickett, N. Rennie, H. Winter, L. Zambonin, L. Landi, A. Jerlich, R. J. Schaur, A. R. Pitt. Detection of phospholipid oxidation in oxidatively stressed cells by reversed-phase HPLC coupled with positive-ionization electroscopy MS. *Biochem. J.* **2001**, *355*, 449.
[46] A. Reis, M. R. M. Domingues, F. M. L. Amado, A. J. Ferrer-Correia, P. Domingues. Radical peroxidation of palmitoyl-lineloyl-glycerophosphocholine liposomes: Identification of long-chain oxidised products by liquid chromatography-tandem mass spectrometry. *J. Chromatogr. B Analyt. Technol. Biomed. Life. Sci.* **2007**, *855*, 186.
[47] E. Maciel, P. Domingues, D. Marques, C. Simões, A. Reis, M. M. Oliveira, R. A. Videira, F. Peixoto, M. R. M. Domingues. Cardiolipin and oxidative stress: Identification of new short chain oxidation products of cardiolipin in in vitro analysis and in nephrotoxic drug-induced disturbances in rat kidney tissue. *Int. J. Mass Spectrom.* **2011**, *301*, 62.

570 [48] A. Reis, P. Domingues, A. J. V. Ferrer-Correia, M. R. M. Domingues. Tandem mass
571 spectrometry of intact oxidation products of diacylphosphatidylcholines: evidence for
572 the occurrence of the oxidation of the phosphocholine head and differentiation of
573 isomers. *J. Mass Spectrom.* **2004**, *39*, 1513.
574 [49] B. A. Wagner, G. R. Buettner, C. P. Burns. Free Radical-Mediated Lipid Peroxidation
575 in Cells: Oxidizability Is a Function of Cell Lipid bis-Allylic Hydrogen Content.
576 *Biochemistry (Mosc.)* **1994**, *33*, 4449.
577 [50] G. R. Buettner. The pecking order of free radicals and antioxidants: lipid peroxidation,
578 alpha-tocopherol, and ascorbate. *Arch. Biochem. Biophys.* **1993**, *300*, 535.
579 [51] E. Brillas, I. Sirés, M. A. Oturan. Electro-Fenton Process and Related Electrochemical
580 Technologies Based on Fenton's Reaction Chemistry. *Chem. Rev.* **2009**, *109*, 6570.
581 [52] A. R. Brash. Lipoxygenases: occurrence, functions, catalysis, and acquisition of
582 substrate. *J. Biol. Chem.* **1999**, *274*, 23679.
583 [53] B. G. Gugiu, C. A. Mesaros, M. Sun, X. Gu, J. W. Crabb, R. G. Salomon. Identification
584 of Oxidatively Truncated Ethanolamine Phospholipids in Retina and Their Generation
585 from Polyunsaturated Phosphatidylethanolamines. *Chem. Res. Toxicol.* **2006**, *19*, 262.
586

587

588

589 **Tab.1** Long chain oxidation products observed in the positive ESI-MS spectra from each
590 oxidized PE (POPE, PLPE and PAPE) with the identification and the indication of the *m/z*
591 values of the $[M+H]^+$ ions

592

593 **Tab.2** Short chain oxidation products observed in the positive ESI-MS spectra from PLPE
594 and PAPE with the identification and the indication of the *m/z* values of the $[M+H]^+$ ions

595

596 **Fig.1** Schematic representation of phospholipid peroxidation initiated by hydroxyl radical,
597 the reactive oxygen species formed during Electrochemical (EC) oxidation. The peroxidation
598 of PAPE (PE 16:0/20:4) is shown as an example. Although the main products and
599 intermediates of oxidation are illustrated for carbons 5 and 8 of the esterified arachidonic
600 acid, the insertion of oxygens can similarly affect other carbon positions of the poly-
601 unsaturated fatty acyl chain. **A**: PAPE bears four bis-allylic carbon atoms on the arachidonoyl
602 chain esterified at sn-2. **B**: Allylic H abstraction and radical rearrangement. **C**: One carbon-
603 centered radical can rearrange along three carbon positions, each of which becomes
604 potentially oxidizable. **D1**: O_2 insertion **D2**: H abstraction from an adjacent PAPE molecule.
605 **E**: Besides 5-hydroperoxy-PAPE, many more primary PAPE hydroperoxydes can be formed,
606 including 7-hydroperoxy-PAPE, 8-hydroperoxy-PAPE. 9-hydroperoxy-PAPE, 10-
607 hydroperoxy-PAPE, 11-hydroperoxy-PAPE, 12-hydroperoxy-PAPE, 13-hydroperoxy-PAPE,
608 15-hydroperoxy-PAPE. These constitutional isomers cannot be distinguished by MS/MS
609 analysis. **F**: One-electron reduction. **G**: Different PAPE poly-hydroperoxides can be formed
610 within a new cycle. **H**: New cycle of H abstraction and O_2 insertion. **I**: Intermediate, highly
611 reactive alkoxy radicals that are formed on the *sn-2* acyl chain can propagate the abstraction

of bis-allylic hydrogens from adjacent PAPE molecules. **L**: Homolytic β-cleavage C5-C6 (*sn-2*). **M**: Homolytic β-cleavage C8-C9 (*sn-2*) and hydroperoxide reduction. **N**: Oxidation of the hydroxide to ketone. **O**: Additional short chain oxidation products can be formed (terminal aldehydes and terminal carboxylic acids in C7, C8, C9, C10 C11, C12, C13, C15). The position of the alkoxyl radical determines the length of esterified *sn-2* acyl chain in the shortened product

Fig.2 Full ESI-MS spectra of the three PE standards object of the present study, before and after the electrochemical oxidation

Fig.3 ESI-MS/MS spectrum in negative ion mode showing the fragmentation of the $[M-H]^-$ ion of hydroxy-hydroperoxy-PAPE (*m/z* 786.5). R_1COO^-: sn1 fatty acid, carboxylate; R_2'COO^-: oxidized sn2 fatty acid, carboxylate; R_2'=C=O: sn2 fatty acid, ketene. The schematic representation of the fragmentation mechanism is also illustrated

Fig.4 ESI-MS/MS spectrum in negative ion mode showing the fragmentation of the $[M-H]^-$ ion of di-hydroperoxy-PAPE (*m/z* 802.5). R_1COO^-: sn1 fatty acid, carboxylate; R_2'COO^-: oxidized sn2 fatty acid, carboxylate; R_2'=C=O: sn2 fatty acid, ketene. The schematic representation of the fragmentation mechanism is also illustrated

Fig.5 ESI-MS/MS spectrum in negative ion mode showing the fragmentation of the $[M-H]^-$ ion of keto-hydroxy-dihydroperoxy-PAPE (*m/z* 832.5). R_1COO^-: sn1 fatty acid, carboxylate;

634 R_2'COO^-: oxidized sn2 fatty acid, carboxylate; R_2'=C=O: sn2 fatty acid, ketene. The
635 schematic representation of the fragmentation mechanism is also illustrated

636

637 **Fig.6** Schematic representation and MS/MS spectrum in positive ion mode showing the
638 fragmentation of the $[M-H]^+$ ion of 1-(palmitoyl)-2-(5-oxopentanoyl)-PE. R_2'=C=O: sn2 fatty
639 acid, ketene. The schematic representation of the fragmentation mechanism is also illustrated

640

641 **Scheme 1** Examples of PAPE long chain oxidation products generated in the electrochemical
642 cell and analyzed by ESI-MS/MS: hydroxy-hydroperoxy-PAPE (A); di-hydroperoxy-PAPE
643 (B); keto-hydroxy-dihydroperoxy-PAPE (C), hydroxy-PAPE (D)

644

645

Figure 1

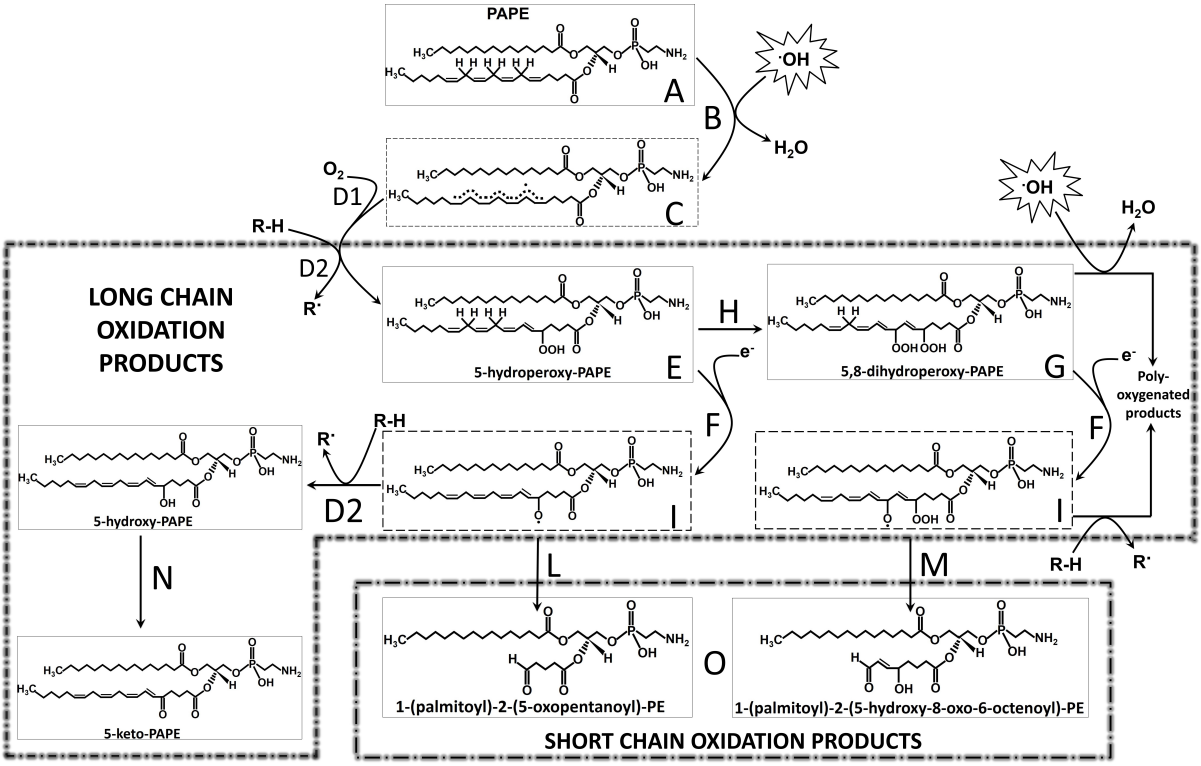
PAPE
A
B
·OH
H2O
C
O2
D1
R-H
D2
R·
LONG CHAIN OXIDATION PRODUCTS
5-hydroperoxy-PAPE
E
H
5,8-dihydroperoxy-PAPE
G
·OH
H2O
e-
Poly-oxygenated products
F
F
R-H
R·
D2
5-hydroxy-PAPE
I
I
N
L
M
R-H
R·
5-keto-PAPE
O
1-(palmitoyl)-2-(5-oxopentanoyl)-PE
1-(palmitoyl)-2-(5-hydroxy-8-oxo-6-octenoyl)-PE
SHORT CHAIN OXIDATION PRODUCTS

Figure 2

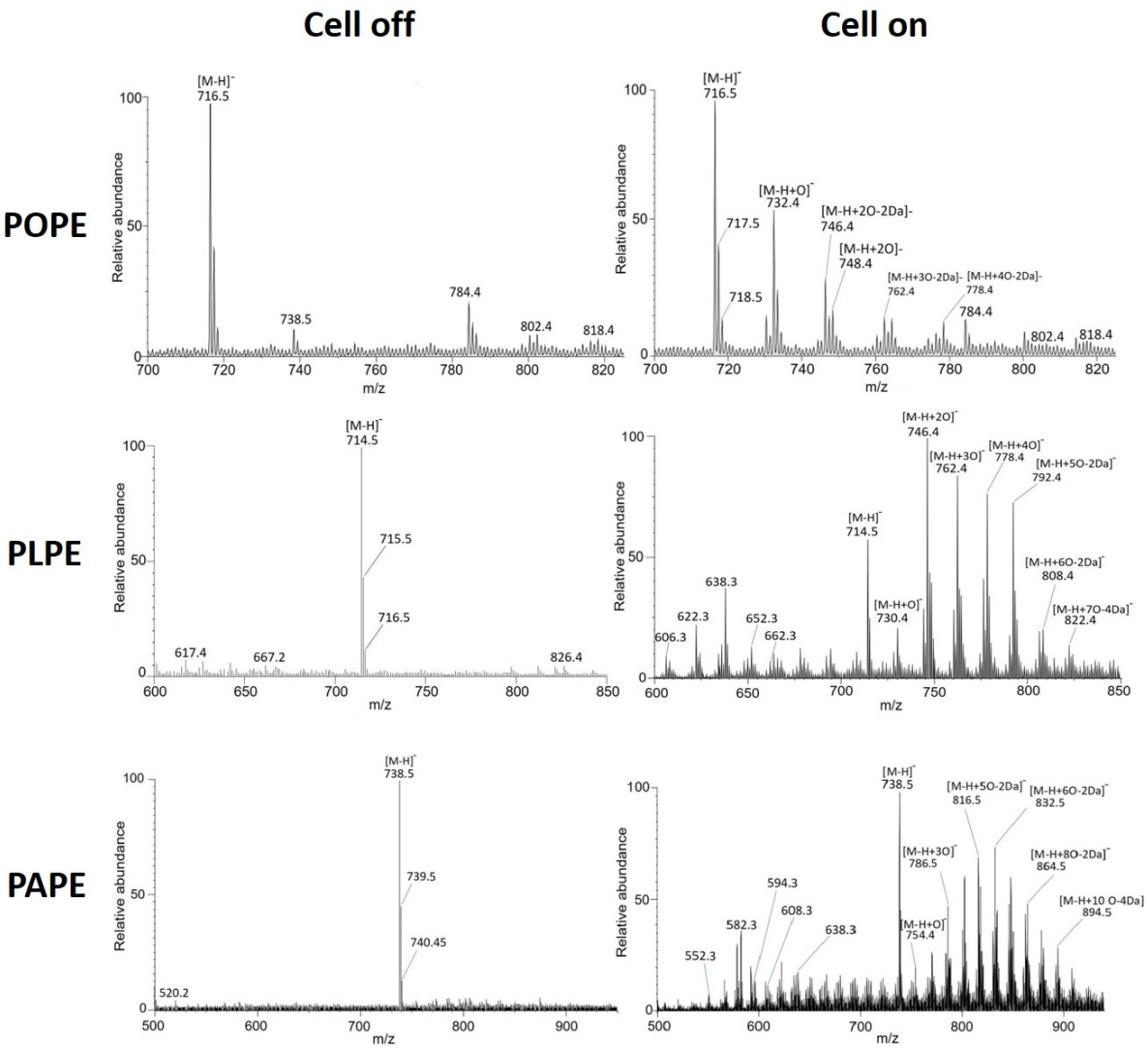
Cell off
Cell on
POPE
PLPE
PAPE
Relative abundance
m/z
[M-H]⁻ 716.5
738.5
784.4
802.4
818.4
717.5
718.5
[M-H+O]⁻ 732.4
[M-H+2O-2Da]- 746.4
[M-H+2O]- 748.4
[M-H+3O-2Da]- 762.4
[M-H+4O-2Da]- 778.4
[M-H]⁻ 714.5
715.5
716.5
617.4
667.2
826.4
[M-H+2O]⁻ 746.4
[M-H+3O]⁻ 762.4
[M-H+4O]⁻ 778.4
[M-H+5O-2Da]⁻ 792.4
[M-H+6O-2Da]⁻ 808.4
[M-H+7O-4Da]⁻ 822.4
[M-H+O]⁻ 730.4
606.3
622.3
638.3
652.3
662.3
[M-H]⁻ 738.5
739.5
740.45
520.2
[M-H+5O-2Da]⁻ 816.5
[M-H+6O-2Da]⁻ 832.5
[M-H+3O]⁻ 786.5
[M-H+8O-2Da]⁻ 864.5
[M-H+10 O-4Da] 894.5
[M-H+O]⁻ 754.4
552.3
582.3
594.3
608.3
638.3

657

658 **Figure 3**

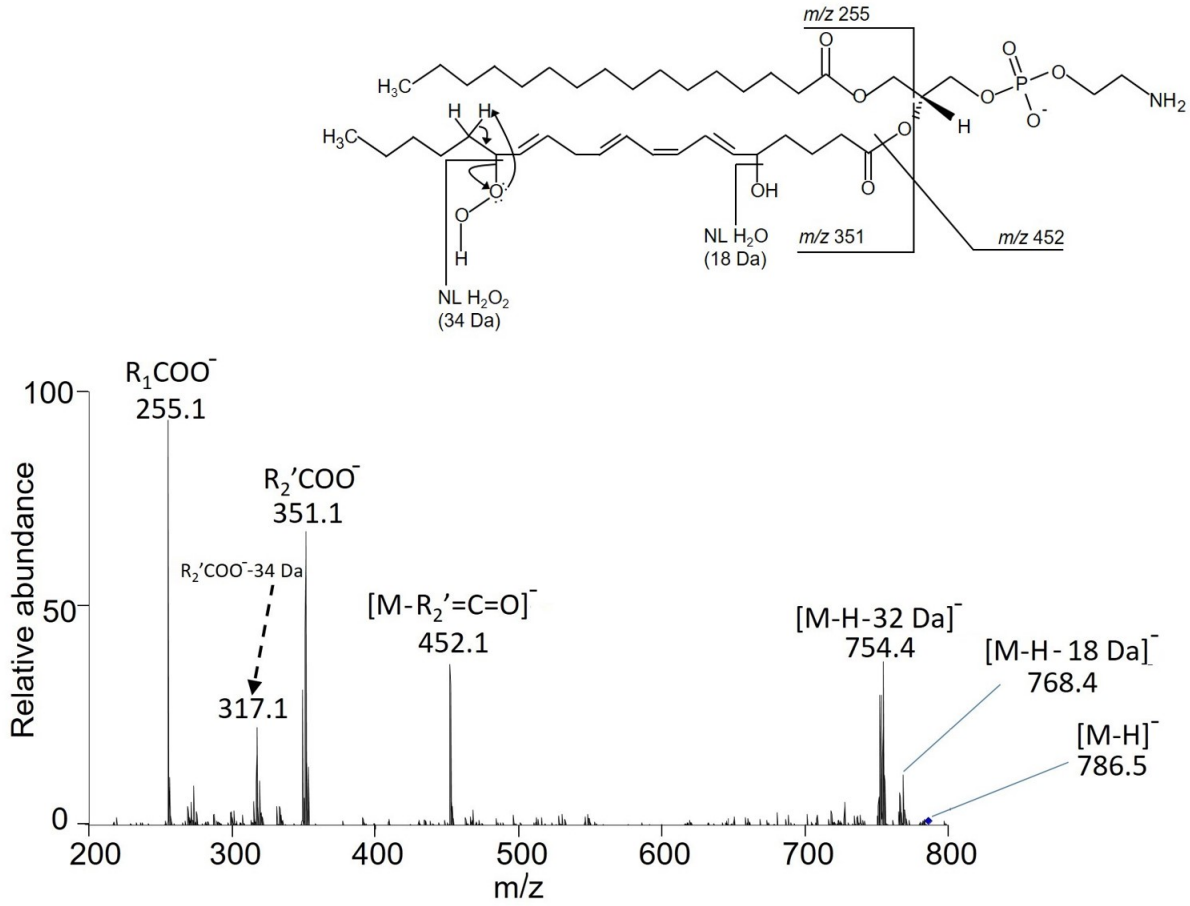

659

660

661

662

663

664 **Figure 4**

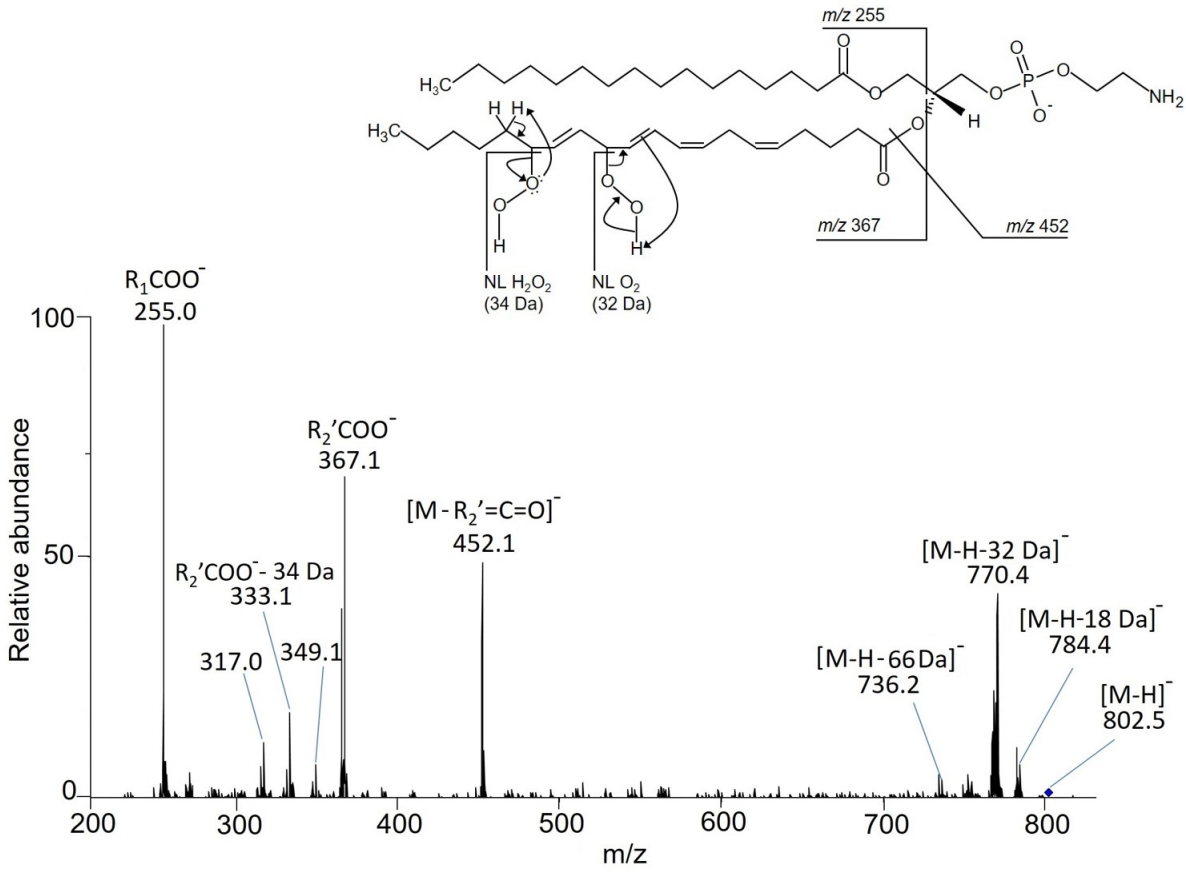

665

666

667

668

669 **Figure 5**

670

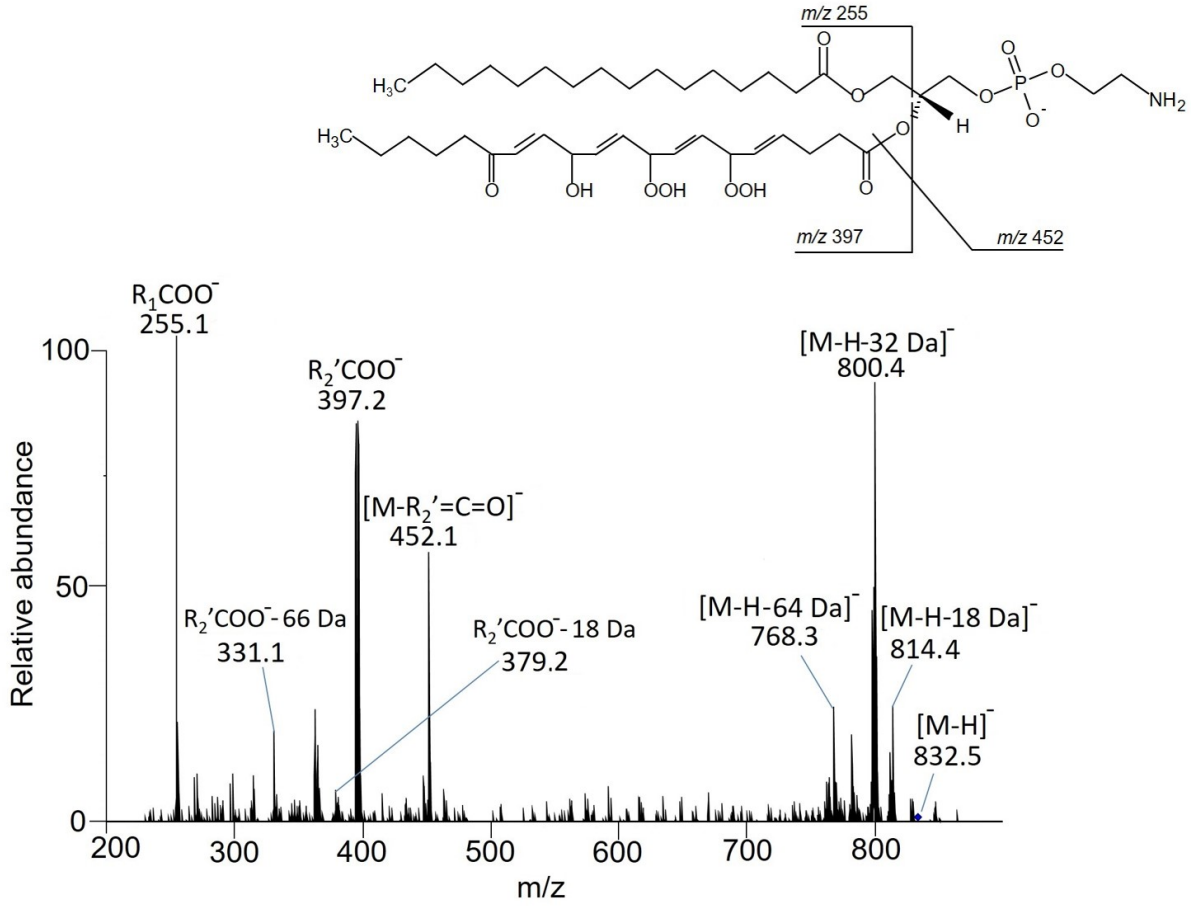

671

672

673

674 **Figure 6**

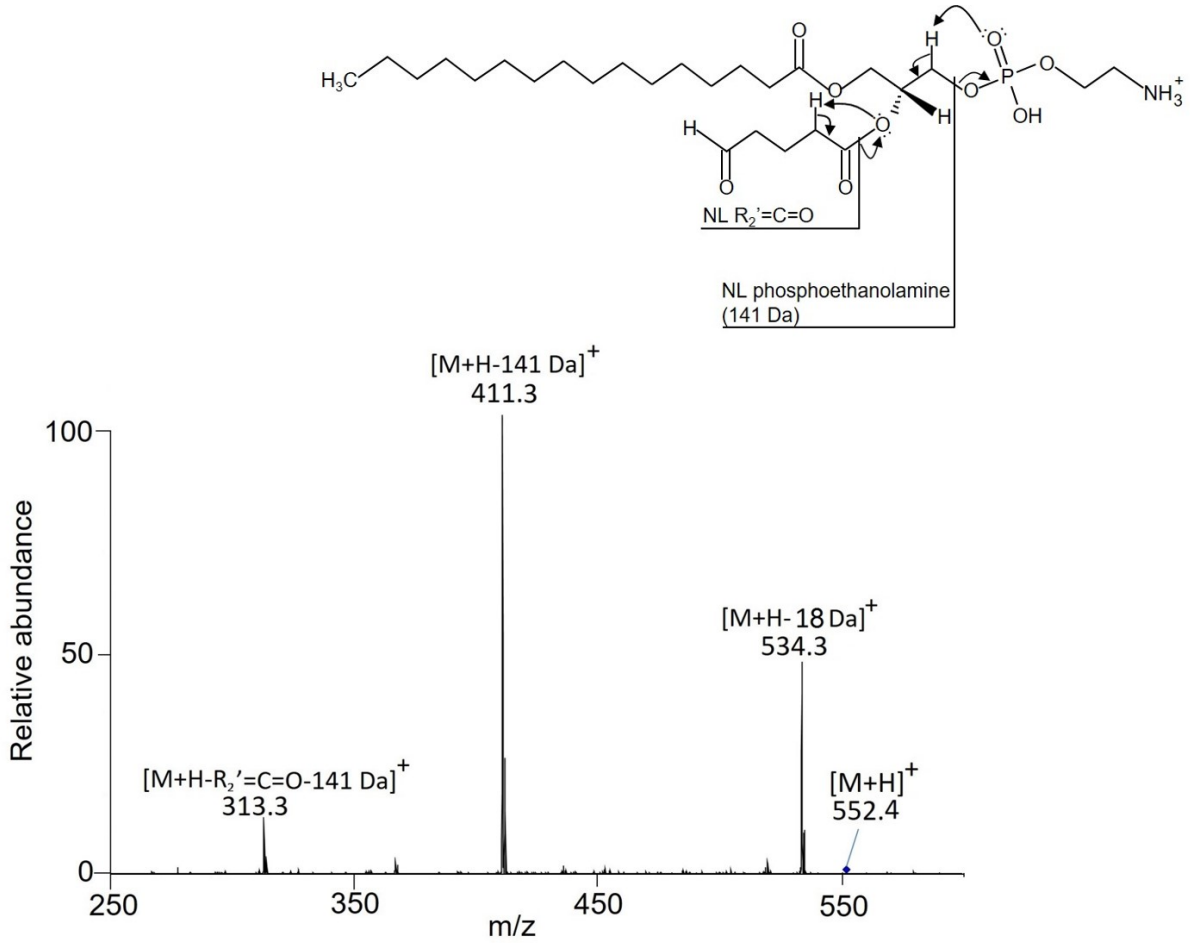

675

676

677

678 Scheme 1

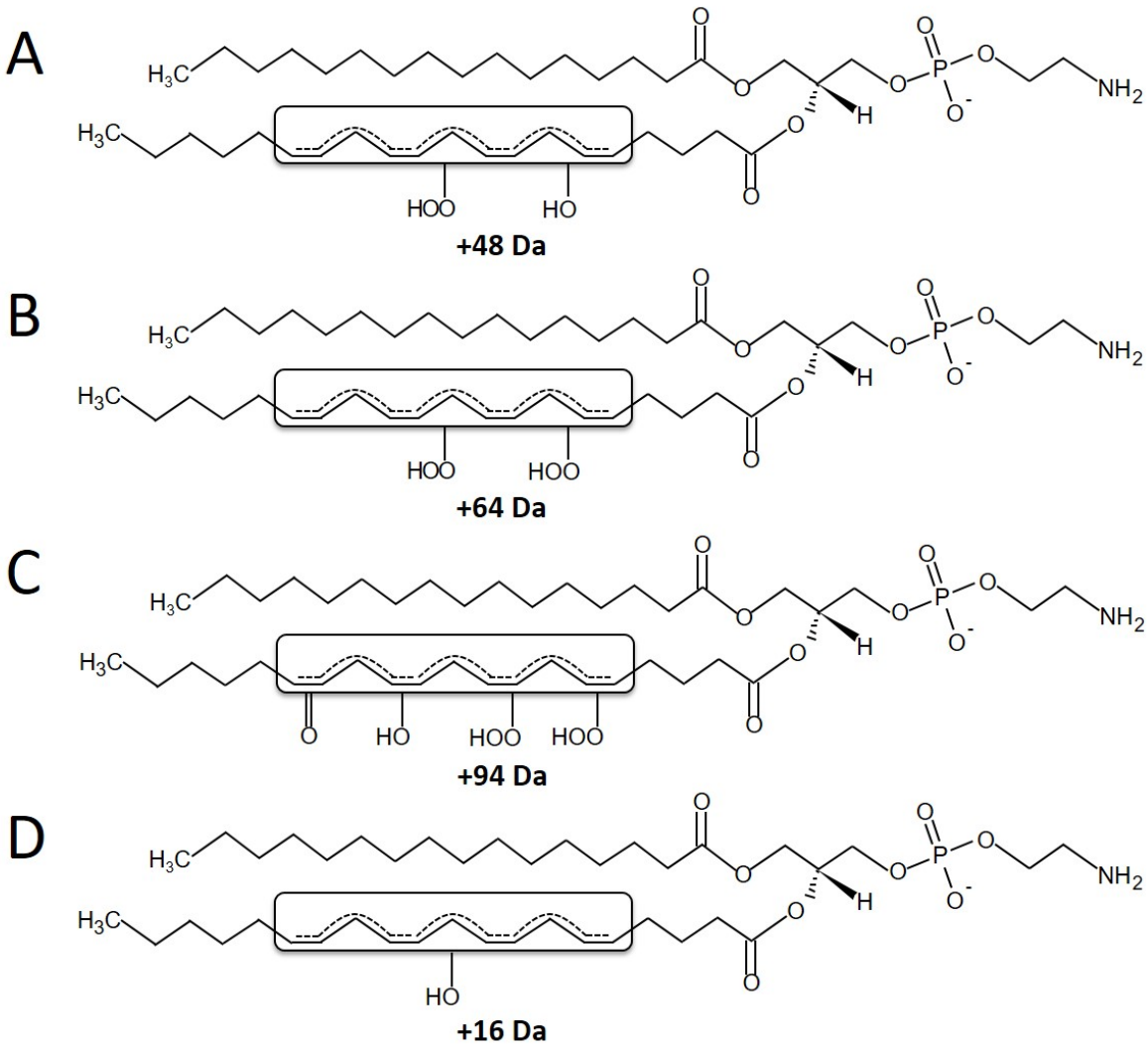

679

680

Table 1

Mass Increment	m/z $[M+H]^+$					
	POPE	Relative abundance	PLPE	Relative abundance	PAPE	Relative abundance
---	718.6	100.00	716.5	64.93	740.5	100.00
14 (+O-2 Da)	732.5	20.44	730.5	32.81	754.5	11.21
16 (+O)	734.6	59.44	732.5	36.20	756.5	13.11
28 (+2O-4 Da)	746.5	15.26	744.4	8.67	768.5	9.16
30 (+2O-2 Da)	748.5	51.12	746.5	36.39	770.5	12.77
32 (+2O)	750.6	47.52	748.5	100.00	772.5	19.70
44 (+3O-4 Da)	762.5	27.50				
46 (+3O-2 Da)	764.5	53.07	762.5	64.18	786.5	32.64
48 (+3O)	766.6	49.01	764.5	73.97	788.5	39.35
60 (+4O-4 Da)	778.5	18.93	776.5	9.88	800.5	12.05
62 (+4O-2 Da)	780.6	28.14	778.5	38.65	802.5	40.95
64 (+4O)	782.5	13.30	780.5	46.60	804.5	50.93
70 (+5O-10 Da)	788.5	12.48				
72 (+5O-8 Da)	790.6	9.91				
76 (+5O-4 Da)	794.6	20.15	792.5	19.61	816.5	21.68
78 (+5O-2 Da)	796.6	15.28	794.5	68.13	818.6	45.78
80 (+5O)			796.5	11.82	820.5	35.64
92 (+6O-4 Da)					832.6	31.62
94 (+6O-2 Da)			810.5	10.72	834.6	47.04
96 (+6O)					836.6	29.20
108 (+7O-4 Da)			824.5	7.85	848.6	34.33
110 (+7O-2 Da)					850.6	32.63
112 (+7O)					852.6	17.39
122 (+8O-6 Da)					862.6	13.55
124 (+8O-4 Da)					864.6	28.27
126 (+8O-2 Da)					866.6	22.48
128 (+8O)					868.6	9.80
138 (+9O-6 Da)					878.5	13.94
140 (+9O-4 Da)					880.6	18.19
142 (+9O-2 Da)					882.6	10.92
156 (+10O-4 Da)					896.6	11.11

686

687

688

689 Table 2

690

Structural feature	GPE	Oxidation product	$[M+H]^+$
Aldehydes	PLPE	1-palmitoyl-2-(9-oxononanoyl)-GPE	608.4
		1-palmitoyl-2-(8-hydroxy-11-oxo-9-undecenoyl)-GPE	650.4
		1-palmitoyl-2-(9-hydroxy-12-oxo-10-dodecenoyl)-GPE	664.4
	PAPE	1-palmitoyl-2-(5-oxopentanoyl)-GPE	552.4
		1-palmitoyl-2-(4-hydroxy-7-oxo-5-heptenoyl)-GPE	594.4
		1-palmitoyl-2-(5-hydroxy-8-oxo-6-octenoic acid)-GPE	608.4
Dicarboxylic acids	PLPE	1-palmitoyl-2-(octanedioic acid)-GPE	610.4
		1-palmitoyl-2-(nonadioic acid)-GPE	624.4
		1-palmitoyl-2-(9-hydroxy-12-oxo-10-dodecenoic acid)-GPE	664.4
		1-palmitoyl-2-(9-hydroxy-10-dodecenedioic acid)-GPE	680.4
	PAPE	1-palmitoyl-2-(pentanedioic acid)-GPE	568.4
		1-palmitoyl-2-(4-hexenedienoic acid)-GPE	580.4
		1-palmitoyl-2-(5-heptenedioic acid)-GPE	594.4
		1-palmitoyl-2-(6-octenedioic acid)-GPE	608.4

691